DOI: 10.21062/mft.2024.095 © 2024 Manufacturing Technology. All rights reserved. http://www.journalmt.com

Statistical Analysis and Machine Learning-Based Modelling of Kerf Width in CO_2 Laser Cutting of PMMA

Ema Vasileska (0000-0003-3937-0546), Ognen Tuteski (0000-0002-0379-0031), Boban Kusigerski (0009-0003-4788-4579), Aleksandar Argilovski (0000-0002-1764-0456), Mite Tomov (0000-0002-4386-7419), Valentina Gecevska (0000-0001-9353-6899)
Faculty of Mechanical Engineering - Skopje, Ss. Cyril and Methodius University in Skopje, Ul. Ruger Boskovic 18, 1000 Skopje, North Macedonia
E-mail: ema.vasileska@mf.edu.mk

Engineering polymers like PMMA have increasingly replaced traditional materials where feasible, with CO_2 laser cutting gaining attention for its high quality and speed in processing these materials. Precise cuts are essential for product accuracy, with kerf width being a key quality attribute for ensuring the final product's quality. This study focuses on the impact of three process variables: stand-off distance, laser power, and cutting speed, on the kerf width in CO_2 laser cutting of PMMA. A full-factorial experiment systematically varies process parameters to understand their individual and interaction effects on the cutting process. The kerf width is measured as an indicator of precision to evaluate the quality of the laser cuts. In order to address the non-linear relationships between these process parameters and kerf width, several machine learning models were utilized. Performance comparisons indicated that the Artificial Neural Network (ANN) model provided the highest accuracy, with R^2 values of 0.98 for the validation dataset and 0.95 for the testing dataset. The optimized ANN model is a robust tool for parameter optimization, determining optimal settings to achieve the desired kerf width and ensure productivity.

Keywords: CO_2 laser cutting, Kerf width, Machine learning, Process modelling

1 Introduction

In recent years, engineering polymers have increasingly replaced traditional materials in various industrial applications, thanks to significant enhancements in their physical properties and performance. Furthermore, the cost efficiency of mass-producing these polymers has improved [1-3]. One such polymer is polymethylmethacrylate (PMMA), known for being a hard, tough, and transparent thermoplastic with a high refractive index and excellent resistance to scratching, aging, and weathering [4]. PMMA is a lightweight, shatter-proof alternative to glass and is widely used in products such as automotive components, optical lenses, sensors, electronics, and biomedical devices [5-11].

Laser cutting of polymers has gained significant attention compared to traditional cutting methods due to its superior product quality, high cutting speed, and reliability [12]. CO_2 laser cutting is particularly effective for processing PMMA, as CO_2 lasers emit at a wavelength of 10.6 μm, which is highly absorbed by PMMA, allowing for efficient cutting with minimal thermal damage to the surrounding material [13]. Additionally, PMMA's low thermal diffusivity ($7 \cdot 10^{-7}\, m^2/s$) and low sublimation point (300°C) further enhance the cutting process, ensuring high-quality cuts and reduced cutting time. The absorbed laser energy is converted into heat, causing the PMMA to sublimate instantly, and the resulting vapor is removed with the help of an assisting gas.

Achieving precise cuts is crucial for maintaining the dimensional accuracy and structural integrity of the final product. The dimensional accuracy as well as the affected surface zone of the cut has been previously researched and compared to other cutting technologies [14]. One important cut quality metric is the kerf, defined as the slot created by material removal, with the width of this slot known as the kerf width (KW) [15]. The kerf width is a critical parameter in laser cutting processes, as it directly impacts the dimensional accuracy of the cut parts and the overall quality of the finished product. Variations in kerf width can lead to deviations from desired dimensions, affecting the fit and function of the components [16-17]. Therefore, controlling and predicting kerf width is essential for ensuring the precision and reliability of laser-cut PMMA components.

The precision and quality of laser cutting are critically influenced by specific input parameters. This relationship has been thoroughly investigated in studies [18-24] that examine the influence of the parameters on cutting region temperature, surface structure, edge quality and operating cost and the published results demonstrate the direct impact of these variables on the cutting performance and material integrity. The process parameters, including stand-off distance (SOD), laser power (P), and cutting speed (v), significantly influence the kerf width during CO_2 laser cutting [25-26]. Selection and setting of the optimal parameter of the laser cutting process to obtain high-quality cuts are of great importance. However, the relationship between these parameters and kerf width is complex and nonlinear, necessitating advanced predictive models for accurate forecasting under varying conditions [27]. Traditional statistical approaches such as Taguchi and response surface methods have been used to select and optimize laser cutting parameters [21], [28]. Nevertheless, these methods have limitations: the Taguchi method does not clearly identify the most influential parameter, and the response surface approach may struggle with highly nonlinear systems. Artificial intelligence (AI) tools, particularly machine learning (ML) techniques, offer a robust alternative due to their ability to handle nonlinear systems, robustness, and generalization capabilities [29]. Consequently, machine learning has emerged as a valuable tool for nonlinear modeling in laser cutting processes [30-31]. Machine learning methods for laser cutting have been explored in literature for process planning [32], optimizing parameters to improve quality [33] and efficiency [34], and minimizing defects [35].

There exist a number of literature works on employing machine learning for predicting kerf attributes. Anjum et al. [36] applied the Gaussian process regression (GPR) technique to predict kerf width and kerf depth in the PMMA micro-milling process with a CO_2 laser machine, using the parameters number of passes, incident energy, laser power, and cutting speed. Kusuma et al. [30] compared the performance of three ML models—support vector regression (SVR), random forest (RF), and extreme learning machine (ELM)—for kerf width prediction in pulsed laser cutting, finding that the RF model performed the best. Alhawsawi et al. [37] investigated the effects of laser power and cutting speed on kerf open deviation (KOD), comparing three ML models: a conventional artificial neural network (ANN), a hybrid neural network–humpback whale optimizer (HWO-ANN), and a hybrid neural network–particle swarm optimizer (PSO-ANN). Najjar et al. [38] used Long Short-Term Memory (LSTM) networks combined with the Chimp Optimization Algorithm (CHOA) to predict kerf quality characteristics in laser cutting of basalt fiber-reinforced polymer composites, considering different process parameters. Additionally, authors have employed monitoring setups on existing machines to indirectly observe kerf attributes [39]. For instance, Ranwu et al. [40] monitored the nanosecond ultraviolet laser cutting of carbon fiber-reinforced polymer using acoustic emission, showing that the emission signal correlates with kerf width in both time and frequency domains. Vasileska et al. [15] used a coaxial camera to monitor kerf width and correlated it to the focusing position. Balarin de Andrade et al. [41] implemented a piezoelectric transducer during the laser cutting process of ceramic, demonstrating that the signals align with the kerf width. The extensive body of research on kerf width modelling in relation to process parameters highlights the critical need for precision in the laser cutting process, ultimately aiming to achieve effective industrial objectives.

This research study contributes to the existing literature on modelling kerf width - a critical quality attribute of the laser cutting process - by examining its relationship with processing parameters when cutting PMMA, a widely used engineering plastic. Utilizing modern machine learning techniques for process modelling, the study begins by detailing a full-factorial experimental design where three variable parameters are defined: stand-off distance, laser power, and cutting speed. The subsequent section describes the measurement procedure for the obtained kerf widths. A statistical analysis is then conducted to understand the influence of these factors on kerf width, followed by a comparison of various machine learning methods for modelling the relationship.

2 Experimental methodology

2.1 Experimental setup

The experiments were performed on a laser machine equipped with a continuous CO_2 laser capable of a maximum output power of 130 W. The laser beam was directed through an optical system of lenses and ultimately focused on the material surface using a focusing lens with a 20 mm diameter. This setup produced a laser spot diameter of 0.13 mm at a focal length of 63 mm. Compressed air was supplied through a 1 mm diameter nozzle, aligned coaxially with the laser beam, to remove molten material and protect the lenses from emitted gases.

2.2 Experimental design

A full-factorial experiment with three repetitions for each combination of factors was conducted on a 3 mm thick PMMA sheet. The variable factors were cutting speed (v), laser power (P), and stand-off distance (SOD), as these significantly influence variations in kerf width as a vital quality attribute of the cut of as shown by empirical studies as well as theory [42]. In the experiment each factor was varied on three levels, selected based on a preliminary study not detailed here for brevity. All the factors' combinations were selected such that the energy input is sufficient to result with a cut. With an SOD of 8 mm, the laser spot was focused on the plate's surface, allowing examination of the kerf width when the laser is focused both above and below the surface. Compressed air was used as assisting gas in the process. The variable factors and their levels are summarized in Table 1.

***Tab. 1** Variable factors and their levels employed in the experiment*

Variable factors	Level		
	Low	Medium	High
Stand-off distance [mm]	7	8	9
Laser power [W]	30	40	50
Cutting speed [mm.s^{-1}]	15	20	25

The experiment consisted of a series of straight-line cuts, each equal to 40 mm in length, performed with a certain combination of parameters. The cutting length of 40 mm was selected to ensure that, after removing the initial and ending part of the cut where the laser movement is accelerated and decelerated, there is a sufficiently long middle region of the cut where the laser operates at its nominal speed providing a consistent cut for accurate measurements. A total of 81 specimen cuts were performed.

2.3 Measurement phase

The cuts were collected in rectangular samples, each containing 9 straight-line cut. An example of rectangular sample obtained from the experiment is shown in Fig. 1 c). Varying kerf widths were produced depending on the process parameters employed for each cut, which were also visually noticeable as can be observed in the Figure. To accurately quantify the kerf width, the cut specimens were measured with an optical microscope from the manufacturer Carl Zeiss, Lena, Germany, equipped with a magnification lens allowing 10 times magnification. The measurement procedure involved using a microscope camera software tool called ImageView (Carestream, Rochester, NY USA) to create a line in the contrast region and measure the distance to the opposite contrast point, which represented the dimension of interest. Three measurements of the kerf width were taken for each cut line at different positions within the region where the cutting speed was constant, as shown on Fig. 1. On the Figure under b) the three measurements are denoted with KW 1, KW 2, and KW 3. The final kerf width used for further analysis and modelling was the average of these three measurements.

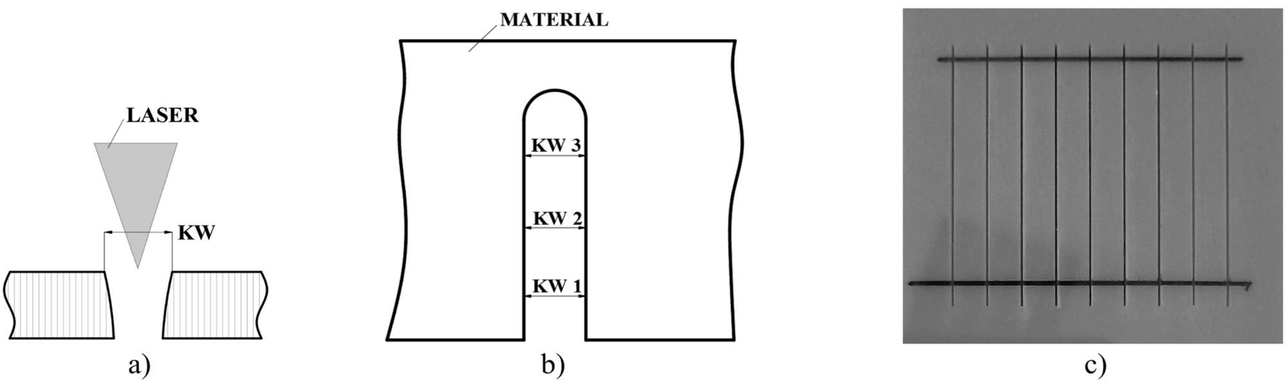

***Fig. 1** Schematic representation of: a) the upper kerf width; b) the three taken measurements of the kerf width; c) rectangular sample with 9 straight-line cuts*

3 Results

3.1 Results from measurement and statistical analysis

The results from the kerf width measurement are shown in Fig. 2. Interval plots are displayed with a 95% confidence interval for the mean kerf width measured in millimetres [mm] for each group. These groups were processed using different laser power and cutting speeds and are presented in three separate graphs based on the stand-off distance (SOD) used in the experiment. A rising trend in kerf width is observed as a function of both the SOD and laser power, while higher cutting speeds result in a narrower kerf width. These trends can be explained by the mechanics of material removal during laser machining of PMMA. Increased laser power contributes to more heat to the workpiece during laser processing, leading to a larger zone of melting and evaporation, as well as larger heat affected zone around the cutting kerf. This is a well-documented phenomenon in experimental works in relevant literature studies. For instance, Son et al. [43] specifically correlated volume energy with kerf dimensions, highlighting the relationship between increased laser power and wider kerf widths. The increase in kerf width with increasing SOD can be attributed to changes in beam focusing and energy distribution when the beam interacts with the material at a different distance. At higher stand-off distances, beam divergence increases, causing a slight increase in laser spot size. Consequently, the heat-affected zone (HAZ) and material removal are greater, leading to a wider kerf width. Regarding cutting speed, the kerf width decreases with increasing cutting speed. This trend is due to the reduced interaction time between the laser beam and the material, which limits the amount of heat input and thus confines the melting and evaporation zones. Consequently, higher cutting speeds result in less material removal and a narrower kerf width. This inverse relationship between cutting speed and kerf width underscores the importance of optimizing cutting parameters for precise laser machining but also keeping in mind the production time and the process productivity.

Fig. 3 presents a contour plot illustrating the variation of kerf width values as a function of the processing parameters. The contour lines are marked with specific kerf width values, providing a clear visual representation of how changes in parameters affect the kerf width. This plot is particularly valuable for optimizing the laser cutting process since by examining the contour lines, one can identify the parameter combinations that yield the desired kerf width.

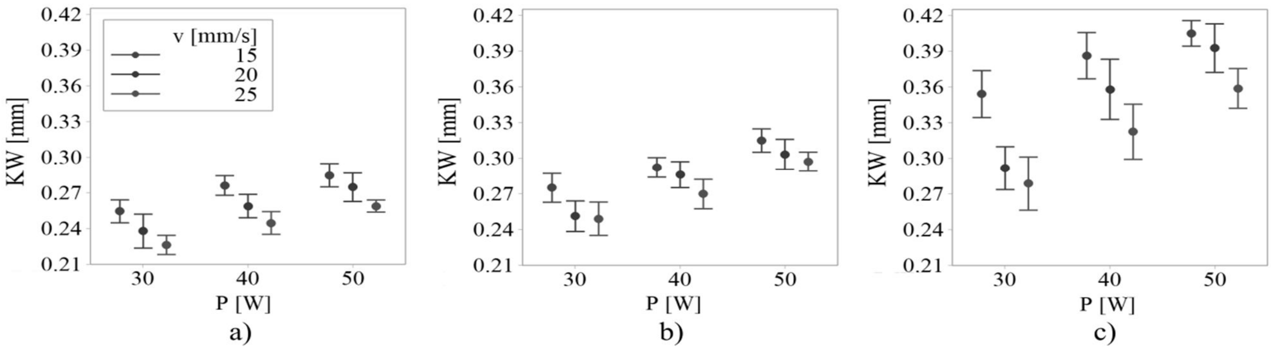

Fig. 2 *Interval plots with 95% confidence interval for the mean of each group of kerf width, where: a) SOD=7 mm; b) SOD=8 mm; c) SOD=9 mm; The colour legend for the v [mm/s] applies to all plots*

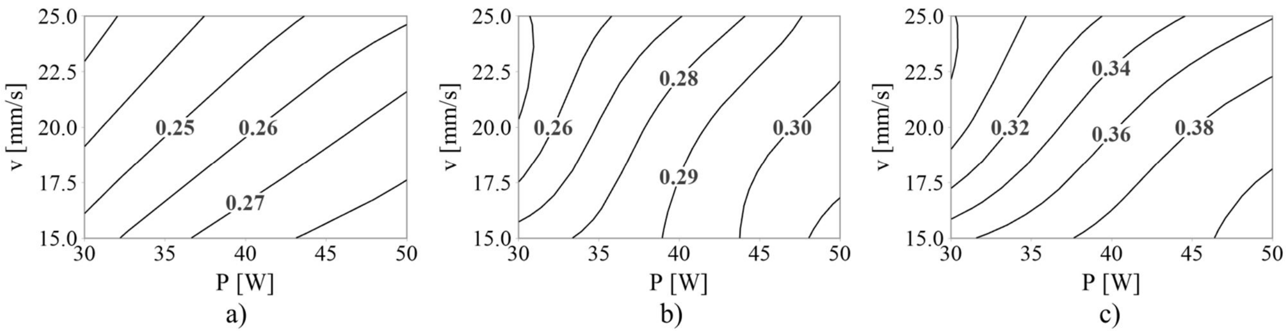

Fig. 3 *Contour plots of the kerf width values as a function of the processing parameters, where: a) SOD=7 mm; b) SOD=8 mm; c) SOD=9 mm; The values of the contour lines are in [mm] unit*

The trends of the kerf width as a function of the three considered factors are illustrated in the main effects plot in Fig. 4 a), highlighting the main trends in kerf width values in relation to the process parameters. As previously concluded and now also depicted in the main effects plot, an increase in P and SOD leads to an increase in kerf width, while an increase in v results in a decrease in kerf width.

In Fig. 4 b), the interaction plot reveals that higher-level interactions between the factors are non-significant. This indicates that each factor independently affects the kerf width, and the combined effects of these parameters at higher levels do not substantially influence the kerf width. Consequently, these higher-level interactions can be excluded from the model for predicting kerf width, as they do not contribute significantly to its variation.

In order to justify the relative importance and significance of process parameters, analysis of variance (ANOVA) was performed on the experimental data and the results are shown in Table 2. ANOVA results confirm the qualitative observations from the main effects plot for KW as it is determined that all parameters are statistically important for KW as indicated by their high F-values and low P-values under the significance threshold level of 0.05. SOD emerged as the most influential factor, followed by laser power and cutting speed. Therefore, to achieve the desired precision in KW, it is essential to select appropriate values for these parameters.

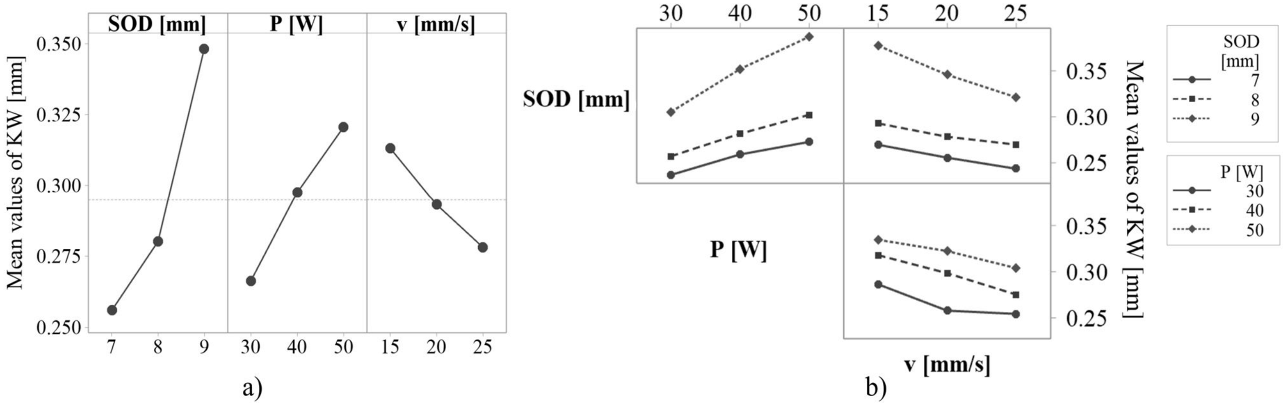

***Fig. 4** a) Main effects plot; b) Interaction plot of the factors on the kerf width*

***Tab. 2** Results from ANOVA analysis*

Source	DF	Adj SS	Adj MS	F-Value	P-Value
Regression	3	0.172408	0.057469	201.40	0.00003
SOD [mm]	1	0.116062	0.116062	406.73	0.00003
v [mm.s^{-1}]	1	0.019032	0.019032	66.70	0.00042
P [W]	1	0.037314	0.037314	130.77	0.00016
Error	77	0.021972	0.000285		
Total	80	0.194380			

3.2 Results from modelling with machine learning methods

Based on the results from the statistical analysis of the interaction between the factors and the output, the three factors without their higher order interactions are considered as inputs in the machine learning model for predicting the kerf width. To test the model's performance, 15% of the dataset was reserved as a testing set. This was done to evaluate the model's ability to generalize to new, unseen data, ensuring its predictions are reliable and not overfitted to the training data. Several regression machine learning models were evaluated to identify the most accurate and reliable model for predicting kerf width. As a metric for evaluating the fitting accuracy of the models, the coefficient of determination (R^2) was used. By comparing their resulting R^2 values for both the training and testing phases, as compared in Fig. 5, it was ensured that the chosen model not only fits the training data well but also generalizes effectively to new, unseen data.

Among the different models tested, the Artificial Neural Network (ANN) model demonstrated the highest R^2 values, achieving 0.98 for the training phase and 0.95 for the testing phase. According to the Fausett [44], the back propagation network with one hidden layer is adequate for a large number of applications. So, in this study, the network with one hidden layer has been used. To optimize the ANN model, configurations with different numbers of neurons were tested. The best performance evaluated with the mean squared error (MSE) was observed with an ANN model consisting of one hidden layer and five neurons. This configuration was chosen not only for its accuracy but also for its balance between performance and complexity. While increasing the number of layers and neurons could potentially improve the results, achieving 98% accuracy was deemed sufficient, avoiding unnecessary complexity in the model. The ANN network has been trained with the experimental data by using Levenberg-Marquadt (LM) algorithms because the LM algorithm is fastest and least memory consuming one [45]. To evaluate the model training process, cross-validation is an excellent method for determining how well the statistical results will apply to a completely new data set. Consequently, five-fold cross-validation was performed in these experiments.

Fig. 6 a) presents a scatter plot of the true versus predicted values of the kerf width using the ANN model, providing a visual assessment of the model's predictive accuracy. The training and testing datasets are distinguished by different colours. The plot demonstrates that the data points are closely aligned around the reference line in its proximity, indicating that the model's predictions closely match the actual values. Furthermore, a histogram depicting the distribution of the residual values for both the training and testing datasets is presented in Fig. 6 b). The residuals represent the differences between the actual measured kerf width and the predicted values from the ANN model, indicating the prediction errors. The histogram illustrates that these errors follow a near-normal distribution, clustering around the zero value. The lack of discernible patterns in the residuals' variation and the absence of significant outliers suggest that the chosen model performs well. This normal distribution of errors indicates that the model's predictions are unbiased and that the errors are randomly distributed, further confirming the model's robustness and reliability.

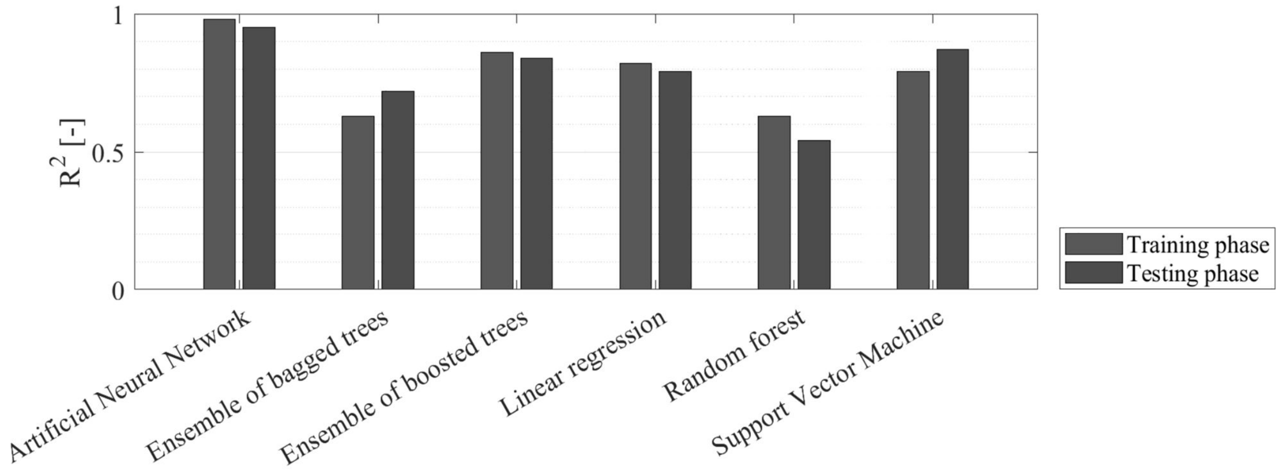

Fig. 5 *Comparison of validation and testing accuracy with R^2 metrics of ML regression models*

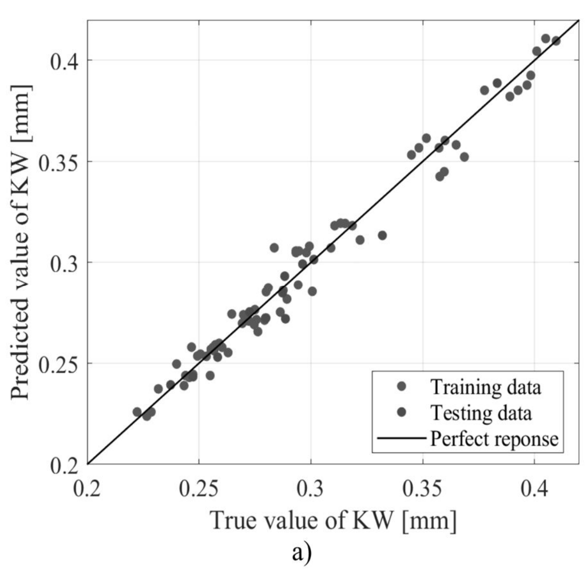

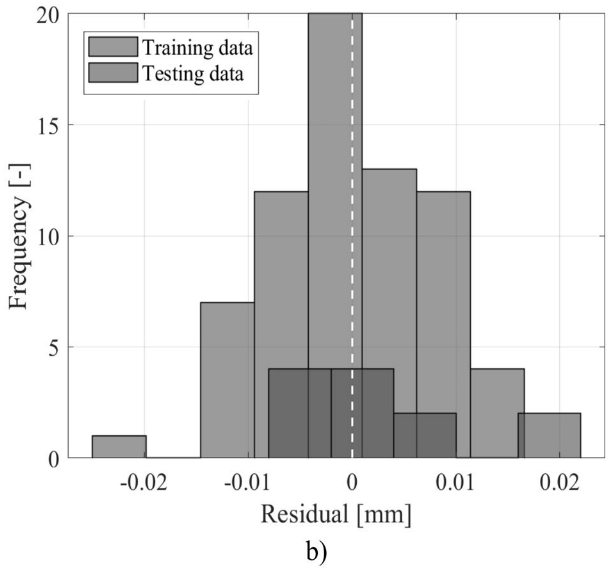

Fig. 6 *a) Scatterplot of true values of KW versus predicted values of KW with ANN model; b) Histogram of the residuals from the ANN modelling*

By utilizing this model, one can determine the optimal set of parameters that yield the desired kerf width while simultaneously considering productivity and energy efficiency. To achieve this, the model can be integrated with an optimization method for appropriate selection of process parameters. This involves defining objective functions that account for not only the precision of the kerf width but also factors like cutting speed, which directly impacts productivity, and laser power, which influences energy consumption. By setting constraints and goals for these parameters, the model can be used to explore the parameter space and identify combinations that meet the desired criteria. The development of integrated ANN with optimization method will be a subject of future research.

4 Conclusions

This research study examined the influence of three significant process variables (stand-off distance, laser power, and cutting speed) on the kerf width, as a quality attribute in the laser cutting process of PMMA. With a designed experiment and conducted statistical analysis it was shown that all three parameters significantly impact the kerf width, where their interaction was non-significant. Of the parameters studied, it was found that the stand-off distance is the most significant, followed by the laser power and the cutting speed. Several machine learning models, suitable for their ability to uncover non-linear relationships, were employed to predict the kerf width as a function of the tested process variables. Their performances were evaluated using the R^2 metric, with the Artificial Neural Network (ANN) model outperforming the others on both the validation ($R^2 = 0.98$) and testing ($R^2 = 0.95$) datasets.

The developed model can be utilized for parameter optimization, enabling the determination of optimal settings that achieve the desired kerf width while considering productivity and energy efficiency. It can be concluded that the proposed approach can be efficiently used for the mathematical modeling and analysis of the effects of process parameters on the cut quality characteristics, as well as contribute to better understanding of the CO_2 laser cutting process. Future research should expand this approach to other materials and thicknesses and explore the integration of real-time monitoring systems to further refine and optimize the laser cutting process.

References

[1] KHOSHAIM, A. B., ELSHEIKH, A. H., MOUSTAFA, E. B., BASHA, M., SHOWAIB, E. A. (2021). Experimental investigation on laser cutting of PMMA sheets: Effects of process factors on kerf characteristics. *Journal of Materials Research and Technology*, vol. 11, pp. 235–246. DOI: https://doi.org/10.1016/j.jmrt.2021.01.012.

[2] KAMAL, A., ELSHEIKH, A. H., SHOWAIB, E. (2020). Pre-Cracking techniques of polymeric materials: An overview. In: *IOP Conference Series: Materials Science and Engineering*, IOP Publishing Ltd. DOI: 10.1088/1757-899X/973/1/012028.

[3] VAKILI-TAHAMI, F., ADIBEIG, M. R., HASSANIFARD, S. (2019). Optimizing creep lifetime of friction stir welded PMMA pipes subjected to combined loadings using rheological model. *Polym Test*, vol. 79, p. 106049. DOI: https://doi.org/10.1016/j.polymertesting.2019.106049.

[4] PAWAR, E. A Review Article on Acrylic PMMA. *IOSR Journal of Mechanical and Civil Engineering (IOSR-JMCE)* e-ISSN, vol. 13, no. 2, pp. 1–04. DOI: 10.9790/1684-1302010104.

[5] ZAFAR, M. S. (2020). Prosthodontic applications of polymethyl methacrylate (PMMA): An update. MDPI AG. DOI: 10.3390/polym12102299.

[6] DÍEZ-PASCUAL, A. M. (2022). PMMA-Based Nanocomposites for Odontology Applications: A State-of-the-Art. MDPI. DOI: 10.3390/ijms231810288.

[7] FEUSER, P. E., et al. (2014). Synthesis and Characterization of Poly(Methyl Methacrylate) PMMA and Evaluation of Cytotoxicity for Biomedical Application. *Macromol Symp*, vol. 343, no. 1, pp. 65–69. DOI: https://doi.org/10.1002/masy.201300194.

[8] MISHRA, S., SEN, G. (2011). Microwave initiated synthesis of polymethylmethacrylate grafted guar (GG-g-PMMA), characterizations and applications. *Int J Biol Macromol*, vol. 48, no. 4, pp. 688–694. DOI: https://doi.org/10.1016/j.ijbiomac.2011.02.013.

[9] HAZIM, A., ABDULJALIL, H. M., HASHIM, A. (2021). Design of PMMA Doped with Inorganic Materials as Promising Structures for Optoelectronics Applications. *Transactions on Electrical and Electronic Materials*, vol. 22, no. 6, pp. 851–868. DOI: 10.1007/s42341-021-00308-1.

[10] ALI, U., Bt. A. KARIM, K. J., BUANG, N. A. (2015). A Review of the Properties and Applications of Poly (Methyl Methacrylate) (PMMA). *Polymer Reviews*, vol. 55, no. 4, pp. 678–705. DOI: 10.1080/15583724.2015.1031377.

[11] SEJC, P., VANKO, B., GABRISOVA, Z. (2021). REW Application Possibilities for the Production of Combined Metal - Plastic Joints. *Manufacturing Technology Journal*, vol. 21, no. 5, pp. 682–690. DOI: 10.21062/mft.2021.082.

[12] HADDADI, E., MORADI, M., KARIMZAD GHAVIDEL, A., MEIABADI, S. (2019). Experimental and parametric evaluation of cut quality characteristics in CO2 laser cutting of polystyrene. *Optik (Stuttg)*, vol. 184, pp. 103–114. DOI: https://doi.org/10.1016/j.ijleo.2019.03.040.

[13] CHOUDHURY, I. A., SHIRLEY, S. (2010). Laser cutting of polymeric materials: An experimental investigation. *Opt Laser Technol*, vol. 42, no. 3, pp. 503–508. DOI: https://doi.org/10.1016/j.optlastec.2009.09.006.

[14] KUCEROVA, L., RACICKY, A., TICHA, I. (2020). Analysis of affected surface zone created by different cutting technologies. *Manufacturing Technology Journal*, vol. 20, no. 6, pp. 785–790. DOI: 10.21062/mft.2020.117.

[15] VASILESKA, E., PACHER, M., PREVITALI, B. (2022). In-line monitoring of focus shift by kerf width detection with coaxial thermal imaging during laser cutting. *International Journal*

of Advanced Manufacturing Technology, vol. 118, no. 7–8, pp. 2587–2600. DOI: 10.1007/s00170-021-07893-8.

[16] DUBEY, A. K., YADAVA, V. (2008). Optimization of kerf quality during pulsed laser cutting of aluminium alloy sheet. *J Mater Process Technol*, vol. 204, no. 1, pp. 412–418. DOI: https://doi.org/10.1016/j.jmatprotec.2007.11.048.

[17] KARATAS, C., KELES, O., USLAN, I., USTA, Y. (2006). Laser cutting of steel sheets: Influence of workpiece thickness and beam waist position on kerf size and stria formation. *J Mater Process Technol*, vol. 172, no. 1, pp. 22–29. DOI: 10.1016/j.jmatprotec.2005.08.017.

[18] SHARIFI, M., AKBARI, M. (2019). Experimental investigation of the effect of process parameters on cutting region temperature and cutting edge quality in laser cutting of AL6061T6 alloy. *Optik (Stuttg),* vol. 184, pp. 457–463. DOI: https://doi.org/10.1016/j.ijleo.2019.04.105.

[19] THAWARI, G., SUNDAR, J. K. S., SUNDARARAJAN, G., JOSHI, S. V. (2005). Influence of process parameters during pulsed Nd:Yag laser cutting of nickel-base superalloys. *J Mater Process Technol*, vol. 170, no. 1, pp. 229–239. DOI: https://doi.org/10.1016/j.jmatprotec.2005.05.021.

[20] ELTAWAHNI, H. A., HAGINO, M., BENYOUNIS, K. Y., INOUE, T., OLABI, A. G. (2012). Effect of CO2 laser cutting process parameters on edge quality and operating cost of AISI316L. *Opt Laser Technol*, vol. 44, no. 4, pp. 1068–1082. DOI: https://doi.org/10.1016/j.optlastec.2011.10.008.

[21] ADALARASAN, R., SANTHANAKUMAR, M., THILEEPAN, S. (2017). Selection of optimal machining parameters in pulsed CO2 laser cutting of Al6061/Al2O3 composite using Taguchi-based response surface methodology (T-RSM). *The International Journal of Advanced Manufacturing Technology*, vol. 93, no. 1, pp. 305–317. DOI: 10.1007/s00170-016-8978-5.

[22] SYKOROVA, L., KNEDLOVA, J., PATA, V., KUBISOVA, M. (2018). Technological Parameters and PMMA Surface Structure. *Manufacturing Technology Journal*, vol. 18, no. 5, pp. 856–860. DOI: 10.21062/ujep/190.2018/a/1213-2489/MT/18/5/856.

[23] ZRAK, A., MESKO, J., SLADEK, A., VICEN, M. (2016). Evaluation of Properties from the Cutting Surface after Applying Laser Beam Technology Using Different Scales of Cutting Speed. *Manufacturing Technology Journal,* vol. 16, no. 6, pp. 1348–1354. DOI: 10.21062/ujep/x.2016/a/1213-2489/MT/16/6/1348.

[24] KUBISOVA, M., PATA, V., SYKOROVA, L., KNEDLOVA, J. (2017). Influence of Laser Beam on Polymer Material. In: *Manufacturing Technology Journal*, Vol. 17, No. 5, pp. 742 – 746. Springer. DOI: 10.21062/ujep/x.2017/a/1213-2489/MT/17/5/742.

[25] ALSAADAWY, M., DEWIDAR, M., SAID, A., MAHER, I., SHEHABELDEEN, T. A. (2024). A comprehensive review of studying the influence of laser cutting parameters on surface and kerf quality of metals. *Springer Science and Business Media Deutschland GmbH*. DOI: 10.1007/s00170-023-12768-1.

[26] YILBAS, B. S. (2008). Laser cutting of thick sheet metals: Effects of cutting parameters on kerf size variations. In: *J Mater Process Technol*, Vol. 201, No. 1, pp. 285 – 290. Elsevier. DOI: https://doi.org/10.1016/j.jmatprotec.2007.11.265.

[27] KHOSHAIM, A. B., ELSHEIKH, A. H., MOUSTAFA, E. B., BASHA, M., SHOWAIB, E. A. (2021). Experimental investigation on laser cutting of PMMA sheets: Effects of process factors on kerf characteristics. In: *Journal of Materials Research and Technology*, Vol. 11, pp. 235 – 246. Elsevier. DOI: https://doi.org/10.1016/j.jmrt.2021.01.012.

[28] NGUYEN, V., ALTARAZI, F., TRAN, T. (2022). Optimization of Process Parameters for Laser Cutting Process of Stainless Steel 304: A Comparative Analysis and Estimation with Taguchi Method and Response Surface Methodology. In: *Math Probl Eng*, Vol. 2022, No. 1, p. 6677586. Hindawi. DOI: https://doi.org/10.1155/2022/6677586.

[29] TERCAN, H., MEISEN, T. (2022). Machine learning and deep learning based predictive quality in manufacturing: a systematic review. In: *J Intell Manuf*, Vol. 33, No. 7, pp. 1879 – 1905. Springer. DOI: 10.1007/s10845-022-01963-8.

[30] KUSUMA, A. I., HUANG, Y.-M. (2022). Performance comparison of machine learning models for kerf width prediction in pulsed laser cutting. In: *The International Journal of Advanced*

Manufacturing Technology, Vol. 123, No. 7, pp. 2703 – 2718. Springer. DOI: 10.1007/s00170-022-10348-3.

[31] BAKHTIYARI, A. N., WANG, Z., WANG, L., ZHENG, H. (2021). A review on applications of artificial intelligence in modeling and optimization of laser beam machining. In: *Opt Laser Technol*, Vol. 135, p. 106721. Elsevier. DOI: https://doi.org/10.1016/j.optlastec.2020.106721.

[32] TERCAN, H., KHAWLI, T., EPPELT, U., BÜSCHER, C., MEISEN, T., JESCHKE, S. (2017). Improving the laser cutting process design by machine learning techniques. In: *Production Engineering*, Vol. 11, pp. 1 – 12. Springer. DOI: 10.1007/s11740-017-0718-7.

[33] ÜRGÜN, S., YİĞİT, H., FIDAN, S., SINMAZÇELİK, T. (2024). Optimization of Laser Cutting Parameters for PMMA Using Metaheuristic Algorithms. In: *Arab J Sci Eng*, Springer. DOI: 10.1007/s13369-023-08627-6.

[34] HWANG, Y.-T., YANG, J.-M. (2024). Laser Cutting Time Estimate for Sheet Metal Parts of Various Geometries by Machine Learning Approach.

[35] IM, D., JEONG, J. (2021). R-cnn-based large-scale object-defect inspection system for laser cutting in the automotive industry. In: *Processes*, Vol. 9, No. 11, p. 2043. MDPI. DOI: 10.3390/pr9112043.

[36] ANJUM, A., SHAIKH, A. A., TIWARI, N. (2023). Experimental investigations and modeling for multi-pass laser micro-milling by soft computing-physics informed machine learning on PMMA sheet using CO2 laser. In: *Opt Laser Technol*, Vol. 158, p. 108922. Elsevier. DOI: https://doi.org/10.1016/j.optlastec.2022.108922.

[37] ALHAWSAWI, A. M., MOUSTAFA, E. B., FUJII, M., BANOQITAH, E. M., ELSHEIKH, A. (2023). Kerf characteristics during CO2 laser cutting of polymeric materials: Experimental investigation and machine learning-based prediction. In: *Engineering Science and Technology, an International Journal*, Vol. 46, p. 101519. Elsevier. DOI: https://doi.org/10.1016/j.jestch.2023.101519.

[38] NAJJAR, I. M. R., SADOUN, A. M., ABD ELAZIZ, M., ABDALLAH, A. W., FATHY, A., ELSHEIKH, A. H. (2022). Predicting kerf quality characteristics in laser cutting of basalt fibers reinforced polymer composites using neural network and chimp optimization. In: *Alexandria Engineering Journal*, Vol. 61, No. 12, pp. 11005 – 11018. Elsevier. DOI: https://doi.org/10.1016/j.aej.2022.04.032.

[39] ARGILOVSKI, A., VASILESKA, E., JOVANOSKI, B. (2023). Enhancing manufacturing efficiency: a lean industry 4.0 approach to retrofitting. In: *Mechanical Engineering-Scientific Journal*, Vol. 41, No. 2, pp. 123 – 129. DOI: 10.55302/mesj23412672123a.

[40] YANG, R., HUANG, Y., RONG, Y., WU, C., LIU, W., CHEN, L. (2022). Evaluation and classification of CFRP kerf width by acoustic emission in nanosecond laser cutting. In: *Opt Laser Technol*, Vol. 152, p. 108165. Elsevier. DOI: https://doi.org/10.1016/j.optlastec.2022.108165.

[41] DE ANDRADE, A. C. B., AGUIAR, P. R., VIERA, M. A. A., ALEXANDRE, F. A., JUNIOR, P. O., DOTTO, F. R. L. (2020). Monitoring of the Ceramic Kerf During the Laser Cutting Process through Piezoelectric Transducer. MDPI AG. DOI: 10.3390/ecsa-6-06529.

[42] STEEN, M. J. (2010). *Laser Material Processing*. Springer, London.

[43] SON, S., LEE, D. (2020). The effect of laser parameters on cutting metallic materials. In: *Materials*, Vol. 13, No. 20, pp. 1 – 15. MDPI. DOI: 10.3390/ma13204596.

[44] FAUSETT, L. V. (1994). *Fundamentals of Neural Networks: Architectures, Algorithms, and Applications*. Prentice-Hall.

[45] SHARMA, A., JOSHI, P. (2023). Comparative analysis of laser profile cutting of Ni-based superalloy sheet using RSM and ANN. In: *International Journal on Interactive Design and Manufacturing (IJIDeM)*. Springer. DOI: 10.1007/s12008-023-01610-3.